



Research Article



## Comparison of Different Nanosuspensions as Potential Ophthalmic Delivery Systems for Ketotifen Fumarate

Saieede Soltani<sup>1,2</sup>, Parvin Zakeri-Milani<sup>3,4</sup>, Mohammad Barzegar-Jalali<sup>4</sup>, Mitra Jelvehgari<sup>1,4\*</sup>

<sup>1</sup> Drug Applied Research Center, Tabriz University of Medical Sciences, Tabriz, Iran.

<sup>2</sup> Student Research Committee, Tabriz University of Medical Sciences, Tabriz, Iran.

<sup>3</sup> Liver and Gastrointestinal Diseases Research Center, Tabriz University of Medical Sciences, Tabriz, Iran.

<sup>4</sup> Department of Pharmaceutics, Faculty of Pharmacy, Tabriz University of Medical Sciences, Tabriz, Iran.

### Article info

#### Article History:

Received: 9 November 2015

Revised: 8 July 2016

Accepted: 11 July 2016

ePublished: 25 September 2016

#### Keywords:

- Ketotifen fumarate
- Nanosuspension
- Transcorneal
- Permeability

### Abstract

**Purpose:** The objective of this study was to develop, characterize, and comparatively investigate the ketotifen fumarate (KF) nanosuspensions (NS<sub>S</sub>) to enhance the permeability of KF.

**Methods:** In the present work, the NS<sub>P</sub> and NS<sub>E</sub> were prepared by double-emulsion solvent evaporation/nanoprecipitation methods with poly (D,L-lactide-co-glycolide) and Eudragit RL100 polymers, respectively. The loading efficiency, particle size, and polydispersity index of prepared different NSs were evaluated with scanning electron microscopy (SEM), X-ray diffraction, differential scanning calorimetry (DSC), Fourier transform infrared spectroscopy (FTIR), and in vitro release and transcorneal permeation. NSs were also compared on the basis of particle size and polydispersity index.

**Results:** Particle size, polydispersity index, and loading efficiency of NS<sub>P1</sub> and NS<sub>E3</sub> showed the best value (158 nm, 117 nm, 0.21, 0.43 and 43%, 95.23%, respectively). SEM showed spherical globules and DSC results showed the reduction in crystallinity. The NS<sub>E3</sub> formulations demonstrated significantly ( $p < 0.05$ ) higher drug release rates than the NS<sub>P1</sub> due to increases in the surface area. Comparative studies showed that NS<sub>E</sub> release and permeability are higher than NS<sub>P</sub>.

**Conclusion:** It is concluded that both NS<sub>P</sub> and NS<sub>E</sub> provide a useful dosage form for the ocular drug delivery which can enhance the permeability of KF.

### Introduction

Eye is the most exclusive organ of the body and a wide range of drug delivery systems are employed to deliver the drug into the eye. Presently, conventional eye drops encompass more than 90% of the marketed ophthalmic formulations. However, after using an eye drop, normally up to 5% of the instilled drug passes the cornea and reaches the intraocular tissues. This happens because of quick and vast precorneal drop loss afforded by blinking and high tear fluid output. To this end, controlled drug delivery to the eye has been suggested as one of the remarkable fields of pharmaceutical research. The major problems associated with conventional systems consist of low drug contact time and poor ocular bioavailability as a result of drainage of drug solution, tear turnover and dilution or lacrimation. Moreover, the anatomical barriers and physiological conditions of the eye are also considerable criteria which dominate designing of drug delivery systems. Numerous novel ocular drug delivery systems such as nanoparticles (NPs), nanoemulsions (NEs), nanosuspensions (NSs) have been developed to achieve higher bioavailability, controlled ocular delivery, patient compliance, and less side effects.<sup>1,2</sup>

NSs and polymeric NPs are more valuable approaches over the current methods in delivering the highly hydrophilic or highly lipophilic molecules across the ocular mucosa. For instance, nanocrystal drug suspensions (NS) entitle an increased dissolution velocity along with saturation solubility of poorly water soluble drugs which is accompanied by an increase in ocular bioavailability.<sup>3</sup>

As a colloidal dispersion of nanosized particles, NSs are stabilized by other excipients like surfactants (as polyvinyl alcohol), viscosity enhancers, or charge modifiers.<sup>4</sup> NSs can also be described as a biphasic system consisting poorly water soluble drug particles dispersed in an aqueous media in which the diameter of the dispersed particles is below 1 $\mu$ m. Size reduction of drug particles conducts to increasing the dissolution rate (enhanced surface area and saturation solubility). The increment in the saturation solubility rate of nanoparticles is related to increase of vapour pressure of the particles.<sup>5</sup> A nanosuspension formulation like this can be prepared by pearl milling, high-pressure homogenization, and precipitation techniques.<sup>6,7</sup>

The precipitation method is the most currently used technique in which the drug is solved in an organic solvent

\*Corresponding author: Mitra Jelvehgari, Tel: +98 41 33392585, Fax: +98 41 33344798, Email: jelvehgri@tbzmed.ac.ir

©2016 The Authors. This is an Open Access article distributed under the terms of the Creative Commons Attribution (CC BY), which permits unrestricted use, distribution, and reproduction in any medium, as long as the original authors and source are cited. No permission is required from the authors or the publishers.

and this solution is admixed with a miscible anti-solvent. In this method, mixing leads to precipitation of drug in the solution, and producing a very fine amorphous or crystalline drug. Precipitation has also been accompanied with the high shear proceeding.<sup>5,8</sup> Several NS formulations have been developed and successfully used for topical ocular drug delivery.<sup>9,10</sup>

Kassem *et al.* formulated NSs for prednisolone, hydrocortisone, and dexamethasone for topical ocular delivery and evaluated them.<sup>11</sup> Studies on the *in vivo* tissue distribution of the glucocorticoid NSs certified remarkably higher levels in anterior chamber tissues in comparison with solution and microcrystalline suspension of similar compounds.<sup>12</sup>

Aksungur *et al.* demonstrated NPs of cyclosporine (CsA) loaded PLGA and /or Eudragit RL-100 and PLGA coated with Carbopol for intensive dry eye syndrome therapy. The ultrafine NPs were supplied with Eudragit RL polymer. It was obtained that the NPs size reduction with Eudragit RL concentration increasing resulted from physicochemical characteristics of the polymer.<sup>13</sup> Mandal *et al.* showed that cloricromene loaded Eudragit RL100 polymeric NPs enhance the ocular bioavailability. They suggested cloricromene-loaded NPs system for clinical trial.<sup>14</sup>

Gupta *et al.* supplied PLGA nanoparticles containing sparflaxacin for ophthalmic delivery using nanoprecipitation technique and showed modified precorneal residence time and ocular penetration for NPs. The improved lyophilized NPs were stable for longer period of time than traditional commercial formulation.<sup>15</sup>

The use of ketotifen fumarate (KF) for the treatment of allergic conjunctivitis behaves as a histamine H1-receptor antagonist, mast cell stabilizer, and eosinophil inhibitor in that it decreases the chemotaxis and activation of eosinophils. Eudragit RL 100 polymers are referred to as ammonium methacrylate copolymers, which are synthesized from acrylic acid and methacrylic acid esters with 10% of functional quaternary ammonium groups.<sup>16</sup> Biodegradable poly (DL-lactic-co-glycolic acid) (PLGA) copolymers have been broadly used as carriers of bioactive molecules.<sup>17</sup> The biocompatibility and biodegradability of PLGA have been proved, and also approved by the FDA for specific human clinical

applications.<sup>18</sup> Polymeric carrier systems using Eudragit and PLGA have been investigated for the ophthalmic release of gentamicin,<sup>19</sup> cloricromene,<sup>20</sup> acetazolamide<sup>21</sup> and non-steroidal anti-inflammatory drugs such as ibuprofen.<sup>22</sup> These carrier systems showed good stabilizing properties and narrow size distribution.

NSs of KF may overcome the problems observed in conventional drops. These nanocarriers may prolong the corneal contact time (higher bioavailability), controlled ocular delivery, rapid penetration of active ingredients, patient compliance, and ocular effect of KF.

The preparation of KF-loaded NS systems and evaluating the effect of polymer type and composition of formulations on the nanocarriers formation have targeted in this study. The feasibility of using the KF-loaded nanoparticulate system as an ocular formulation was demonstrated through extensive characterization of the size, charge, loading efficiency, drug release, and transcorneal permeability.

## Materials and Methods

### Materials

For this study, the KF was supplied by Behansar Co. (Iran). Eudragit RL 100 was kindly a gift from Akbarie Co. (from RÖhm Pharma GmbH, Weiterstadt, Germany). PLGA polymer Resomer® 502 H (MW 7000-17000) was purchased from Sigma-Aldrich (Sigma-Aldrich Co. US). Polyvinyl alcohol (MW 72000), D-mannitol, dichloromethane (DCM), ethanol, sodium chloride, calcium chloride, and potassium chloride were obtained from Merck (Germany). All solvents and reagents were of analytical grade. Commercial eye drop (Zaditen®, 0.025%) was purchased from Thea pharma (France).

### Methods

#### Preparation of KF-NS<sub>P</sub> and KF-NS<sub>E</sub>

Two nanocarriers, NS<sub>P</sub> (Nanosuspension of PLGA polymer) and NS<sub>E</sub> (Nanosuspension of Eudragit RL100 polymer) were produced using PLGA and Eudragit RL 100, described polymers.<sup>23</sup> Briefly, NS<sub>E</sub> and NS<sub>P</sub> were prepared by nanoprecipitation method and double emulsion solvent evaporation technique (W<sub>1</sub>/O/W<sub>2</sub>) at different drug to polymer ratios, respectively (Table 1).

**Table 1.** Selected preparation parameters and their investigated range

Preparation parameter	Selected formulation		Investigation range	
	NS <sub>P1</sub>	NS <sub>E3</sub>	NS <sub>P</sub>	NS <sub>E</sub>
Polymer type	PLGA	Eudragit RL100	PLGA	Eudragit RL100
Drug to polymer ratio	1:5	1:15	1:5 - 1:10	1:7.5 - 1:15
Amount of drug (mg)	10	10	10	10
Concentration of polymer (mg/ml)	5	12.5	5-10	6.25-12.5
PVA (1%w/v)/ NaCl (0.8 %w/v) (ml)	25	-	25	-
PVA (1%w/v) (ml)	-	25	-	25
Theoretical drug content (%)	16.67	6.25	9.10-16.67	6.25-11.76
Mean drug entrapped (%±SD)	10.58±0.85	9.52±6.35	4.07-10.58	9.39-9.52
Drug loading efficiency (%±SD)	43.00±8.00	95.23±8.45	43-55	93.95-95.23
Mean particle size (nm)	158±2.24	117±16.00	158-754.6	117-182
Zeta Potential (mV±SD)	-3.30±3.21	+13.40±0.28	-3.30 - -2.99	+6.58-13.40
Polydispersity Index (±SD)	0.21±0.29	0.43±0.18	0.21-0.83	0.34-0.73

Formulation of KF-NS<sub>P</sub>: An aqueous 0.5 % w/v KF solution was added to 10 ml PLGA in organic solvent (dichloromethane) by using an ultrasound probe (Hielscher, UP200H, amplitude 80%) in an ice bath for 3 min. This solution was added drop by drop using syringe needle to 25 ml aqueous phase of PVA (1% w/v), NaCl (0.8% w/v) and sonicated for 3 min. Then this emulsion was diluted in 50 ml distilled water. The organic solvent was allowed to evaporate at room temperature under magnetic stirring and NS<sub>P</sub> were collected by centrifugation (Eppendorf, Centrifuge 5810 R, Germany) at 12000 rpm, 4°C for 60 min and washed and freeze-dried.

Formulation of KF-NS<sub>E</sub>: KF and Edragit RL 100 were dissolved in 12 ml ethanol. The solution was mixed with 25 ml of 1% w/v PVA aqueous solution using ultrasound probe (Hielscher, UP200H) for 3 min. Then the mixture of drug and polymer was diluted in 50 ml distilled water. Finally, the resulted nanosuspension was stirred at room temperature to extract the organic solvent. NS<sub>E</sub> was separated under the same conditions of NS<sub>P</sub>. Prepared NPs were mixed with 10ml 5% w/v mannitol solution as a cryoprotectant and then lyophilized.

### Characterization of NS<sub>P</sub> and NS<sub>E</sub>

#### Particle size and zeta potential

Particle size and zeta potential of freshly prepared NS<sub>P</sub> and NS<sub>E</sub> were determined by Dynamic Light Scattering (Malvern, UK) using a Zetasizer. The zeta potential is used to measure the electric charge at the surface of the particles, showing the physical stability of colloidal systems. For this study, the formulated NS<sub>P</sub> and NS<sub>E</sub> were diluted with distilled water. Visual observations were made immediately after dilution for evaluation of NS<sub>P</sub> and NS<sub>E</sub> efficiency, appearance (transparency), phase separation, and precipitation of drug. The polydispersity index of the resulting NS<sub>P</sub> and NS<sub>E</sub> were determined by dynamic light scattering with Zeta sizer.

#### Morphology

The outer macroscopic structure of NS<sub>P</sub> and NS<sub>E</sub> were investigated by scanning electron microscopy (SEM). SEM (MIRA3 TESCAN, Czech Republic) was used to examine the surface morphology of Eudragit and PLGA nanoparticles. The samples were stationed on a metal stub with a double adhesive tape and coated with the platinum/palladium alloy under the vacuum.

#### Drug loading and production yield of NS<sub>P</sub> and NS<sub>E</sub>

To determine the amount of drug loaded in prepared nanocarriers, NS<sub>P</sub> and NS<sub>E</sub>, the supernatant was UV analyzed for the unloaded drug at wavelength 298 nm. Calibration curve was performed by means of KF in 1% PVA aqueous solution. The drug loading efficiency was determined using the following equations:<sup>24</sup>

$$\text{Drug loading efficiency} = \frac{\text{Total amount of drug} - \text{unincorporated drug amount}}{\text{Total amount of drug}} \times 100$$

#### Evaluation of physical state and polymer-drug interaction of NS<sub>P</sub> and NS<sub>E</sub>

Physical state and polymer-drug interaction of NS<sub>P</sub> and NS<sub>E</sub> were examined by XRD, DSC and FTIR analyses.

X-ray diffraction (XRD): XRD analysis was performed using Bruker Axs, D8 Advance diffractometer with nickel-filtered CuK $\alpha$  radiation (operating at 40KV, 20mA). The scanning rate was 4 °C/min over a 2 $\theta$  range of 10°-90°.

Differential scanning calorimetry: Differential scanning calorimetry (DSC) (Shimadzu, Japan) measurements were carried out on drug, polymers and different formulations. The weighed samples were put in aluminum pans and scanned for 30°C-300°C with heating rate of 10°C/min.

Fourier transform infrared spectroscopy: The Fourier transform infrared spectroscopy (FT-IR) spectra for KF loaded nanocarriers, blank NPs, polymer and drug were obtained by a computerized FT-IR (Bruker, Tensor 27, and USA) operating in the scanning wavenumber range of 400-4000 cm<sup>-1</sup> at 1 cm<sup>-1</sup> resolution.

#### In vitro release study

##### In vitro release

*In vitro* release experiments were performed on the NS<sub>P</sub> and NS<sub>E</sub> using dialysis bag diffusion method.<sup>20</sup> Fifty milligrams of particles were suspended in 4 ml SLF (simulated lacrimal fluid) buffer (pH 6.8) in the dialysis bag (cutoff 12,000 Da), which was immersed in 300 ml of the same buffer as dissolution medium. The medium was preheated to 32±1°C and stirred at 100 rpm. At preset intervals, 3.5 ml of medium were withdrawn and replaced with 3.5 ml of fresh SLF to keep the sink condition. The amount of KF in the samples was determined by UV spectrophotometer (Shimadzu, Japan) analysis at wavelength 298 nm. The experiments were repeated for each formulation in triplicate.

#### Ex-vivo transcorneal permeation studies

The *in vitro* permeation study of the KF-loaded NS<sub>P</sub> and NS<sub>E</sub> through the bovine cornea was performed using Franz diffusion cell at 32 °C. Freshly obtained scleral layer was mounted between the donor and the recipient compartments. The nanocarriers suspended in 5 ml distilled water were placed on the epithelial faced surface and the compartments were clamped together. The NS<sub>P</sub> and NS<sub>E</sub> was stationed on the cornea, and the opening of the donor compartment was sealed with a glass coverslip and soaked with simulated lacrimal fluid (SLF, composition: 8.3 g of NaCl, 0.084g of CaCl<sub>2</sub>·2H<sub>2</sub>O, 1.4g of KCl, and distilled deionized water to 1000 mL). The recipient compartment was filled with 22-25 ml SLF at pH 6.8 and stirred with a magnetic bead at 200 rpm.<sup>25</sup> Three milliliters of the sample were withdrawn at predetermined time intervals and analyzed for drugs at 298 nm.

Permeability coefficient was calculated using the following equation:

$$K_p = \frac{J_{ss}}{C_0}$$

Where  $J_{ss}$  is the steady state flux per unit area,  $K_p$  is the permeability coefficient for a given solute in a given vehicle ( $\text{cm h}^{-1}$ ), and  $C_0$  is the concentration of the solute in the donor compartment.

### Statistical analysis

Where appropriate, all results were evaluated using a one-way ANOVA or t-test at the 0.05 level of error.

### Results & Discussion

The composition of  $NS_P$  and  $NS_E$  formulations are listed in Table 1, where the amount of the different compounds is expressed as % (w/w). As shown in the table,  $NS_P$  was prepared by using PLGA and DCM as the organic phase, PVA as stabilizer and sodium chloride as osmosis pressure agent.<sup>26</sup>  $NS_E$  was produced by using Eudragit RL100 and ethanol as organic phase and PVA as emulsifier. Both formulations,  $NS_P$  and  $NS_E$ , were loaded with the same amount of KF (10 mg)

and stabilized with the same surfactant in the same concentration (1% w/v).

In the  $NS$ , water was used as an anti-solvent whereas polyvinyl alcohol was used as the surfactant. Nanoprecipitation occurs at the interface of the organic phase (ethanol) and anti-solvent phase (water) due to diffusion of the solvent by forming local disturbances followed by precipitation of nanoparticles which were governed by surfactant system.

Under the sonication, the mixture of ethanolic was injected into the aqueous phase so the nanosuspension (polymeric solutes become aggregated to produce nanosized particles) was formed by precipitation with diluted organic solution in the aqueous phase leading to the production of nanoparticles. The sonication was operated for several minutes to let the system reach equilibrium. The solvent displacement method for fabrication of  $NS$  was adopted from the nanoprecipitation method applied for polymeric nanoparticles. The organic phase (O) was poured into an aqueous phase (W) containing a surfactant to yield nanosuspension.<sup>4</sup>

The highest loading efficiency for  $NS_P$  and  $NS_E$  formulations were 43% and 95.23%, respectively. The results showed that the drug was uniformly distributed throughout the  $NS_E$  formulations (Table 2).

**Table 2.** Comparison of various release characteristics, flux and permeability coefficient of KF from different NPs formulations and commercial<sup>®</sup> drop

Formulation code	<sup>a</sup> Rel <sub>0.25</sub> (%)	<sup>b</sup> Rel <sub>8</sub> (%)	<sup>c</sup> DE	<sup>d</sup> T <sub>50%</sub> (min)	<sup>e</sup> f <sub>1</sub>	<sup>f</sup> Flux (mg/cm <sup>2</sup> .min)*10 <sup>-3</sup>	<sup>g</sup> K <sub>p</sub> (cm/min) *10 <sup>-4</sup>
NS <sub>P1</sub>	15.81±3.04	82.57±4.87	74.49	248.84	44.68	0.2	5.82
NS <sub>P2</sub>	12.30±0.52	65.15±7.75	62.72	352.61	54.72	0.06	3.44
NS <sub>P3</sub>	10.67±0.26	58.77±8.53	54.04	383.74	63.38	0.06	4
NS <sub>E1</sub>	30.67±1.54	65.51±4.10	61.28	93	49.24	0.6	10.7
NS <sub>E2</sub>	55.74±5.28	80.31±3.48	77.77	45.64	28.19	0.6	16.78
NS <sub>E3</sub>	65.14±1.44	88.82±3.33	85.88	46.61	20.22	0.5	17.30
KF drop <sup>®</sup>	97.77±0.00	101.62±1.81	101.03	8.31	0	0.1	28.99

<sup>a</sup> Rel<sub>0.25</sub> = amount of drug release after 0.25 h; <sup>b</sup> Rel<sub>8</sub> = amount of drug release after 8 h; <sup>c</sup> DE = dissolution efficiency; <sup>d</sup> t<sub>50%</sub> = dissolution time for 50% fractions; <sup>e</sup> f<sub>1</sub> = Differential factor (0<f<sub>1</sub><15), <sup>f</sup> flux and <sup>g</sup> permeability coefficient.

Particle size diameter (Z-Ave), polydispersity index (PI), and zeta potential of  $NS_P$  and  $NS_E$  were determined just after preparation (reported in Table 1). Freshly prepared  $NS_{P1}$  showed a Z-Ave of 158 nm (0.21 PI) and a zeta potential of -3.30 mV while freshly prepared  $NS_{E3}$  presented a Z-Ave of 117 nm (0.43 PI) and a zeta potential of +13.40 mV. As can be observed,  $NS_P$  and  $NS_E$ , showed negative and positive zeta potential values, respectively. The positive zeta potential of  $NS_E$  may a longer residence time of NPs on the corneal surface. As shown in Table 2, freshly prepared  $NS_{P1}$  was well homogeneously dispersed with reduced particle size and PI, compared to the  $NP_{E3}$  that was briefly homogeneously dispersed. However, Table 2 clearly shows that  $NS_E$  was less stable than the  $NS_P$ . The low stability of this formulation ( $NS_E$ ) was also confirmed by the increasing of polydispersity index value from 0.34 to

0.73. On the basis of PDI, we found that KF-loaded  $NS_P$  was better than KF-loaded  $NS_E$ . A higher value of polydispersity index indicates a broad particle size distribution.<sup>27</sup>  $NS_P$  and  $NS_E$  data were confirmed by SEM images (Figure 1).

SEM is used to assess the microscopic surface morphology of the formulations. Prepared formulations were present in the form of a rough surface which might have led to the enhanced

dissolution rate.<sup>27</sup> Moreover, the particle showed a satisfactory regular spherical shape in the case of  $NS_P$ , which is probably the reason for its best results even in the dissolution.

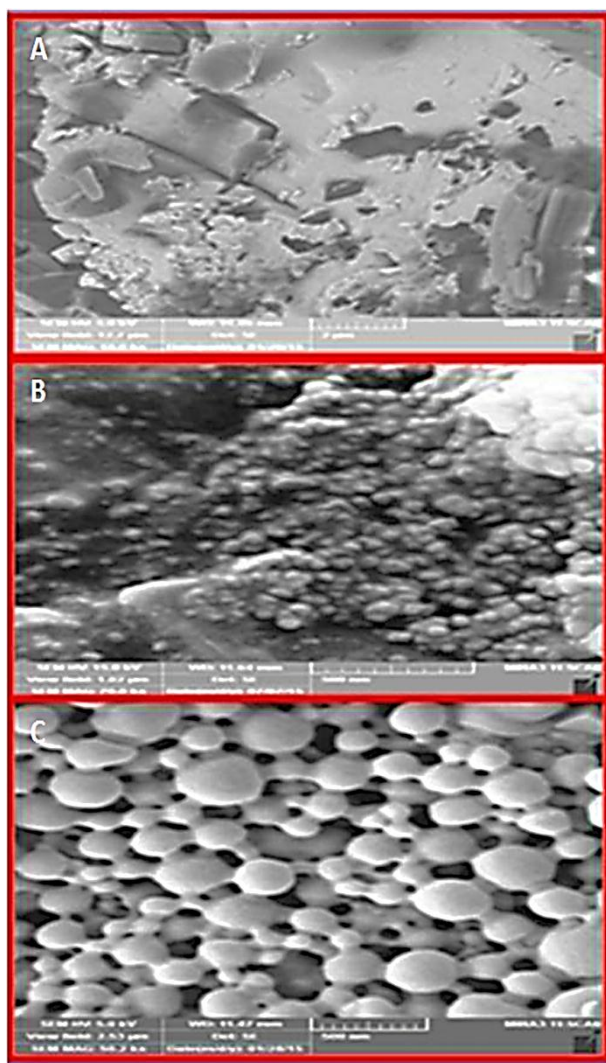


**Figure 1.** SEM images of KF (A); NS<sub>E3</sub> (KF:EU) 1:15 ratio (B); NS<sub>P1</sub> (KF:PLGA) 1:5 ratio (C) at 1000x magnification.

The influence of preparation method on the KF degree of crystallinity and melting point was evaluated by DSC characterization of NS<sub>P</sub> and NS<sub>E</sub>. The freeze dried drug loaded NS<sub>E</sub> exhibited a sharp melting endotherm at an onset temperature of 197.69 °C, a peak temperature of 201.09 °C, and a heat of fusion of 176.14 J/g (Figure 2). The freeze dried drug loaded NS<sub>E</sub> showed a broad endothermic transition at an onset of 216.68 °C, a peak at an onset of 197.93°C, and a peak at 213.96 °C (from F<sub>1</sub> to F<sub>3</sub>). Eudragit RL 100 and PLGA polymers are found as an utterly amorphous form with a glass transition temperature (T<sub>g</sub>) of about 60°C.<sup>28</sup> No fusion peak or phase transition was observed in the amorphous polymer, apart from a broad signal around 55–60°C owing to a partial loss of residual humidity.<sup>29</sup> The thermal behavior of the freeze dried NPs proposed that the polymer prevented the melting of drug crystals. The ionic interaction may have occurred in the NPs as observed for the KF and Eudragit RL 100 system.<sup>30</sup> However, the NPs of KF shows drug melting peak. The thermal profile comparison between NS<sub>P</sub> and NS<sub>E</sub> KF confirmed that the

solid state transition that occurred during NS preparation did not influence the drug behavior.

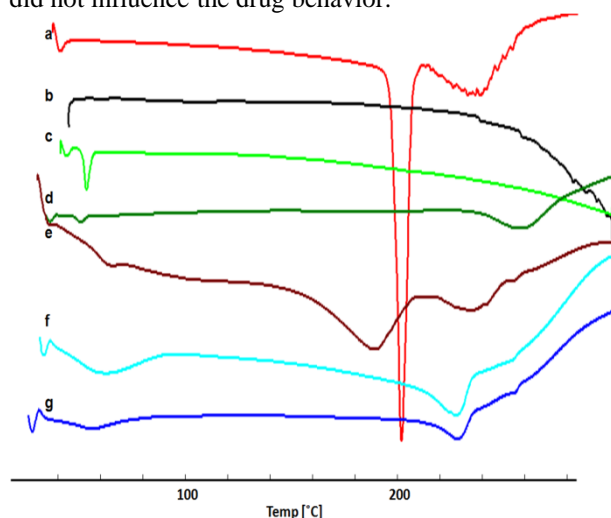


**Figure 2.** DSC thermogram of KF (a); PLGA (b); NS<sub>P1</sub> (KF:PLGA) 1:5 ratio (c); blank NS<sub>P1</sub> (d); Eudragit RL100 (e); NS<sub>E3</sub> (KF:EU) 1:15 ratio (f); blank NS<sub>E3</sub> (g), respectively.

In the XRD, spectra are obvious and the NS<sub>P</sub> with lower polymer concentration would show similar peaks as the blank NS<sub>P</sub>. For NS<sub>P</sub>, some of the identifying peaks for KF are detectable at a high concentration of polymer; though these peaks hold very low intensity due to the presence of lower concentration of drug in the sample compared to pure KF sample (Figure 3). Eudragit RL polymer is completely amorphous in nature, and entrapment of crystalline KF (sharp intense peaks as seen in Figure 3) into the polymeric NS<sub>E</sub> reduced its crystallinity to a greater extent. This is evident from the disappearance of most peaks in the NS<sub>E</sub> compared to the drug. There may also be the possibility of overlapping of drug peaks by the background diffraction pattern of the amorphous structure.

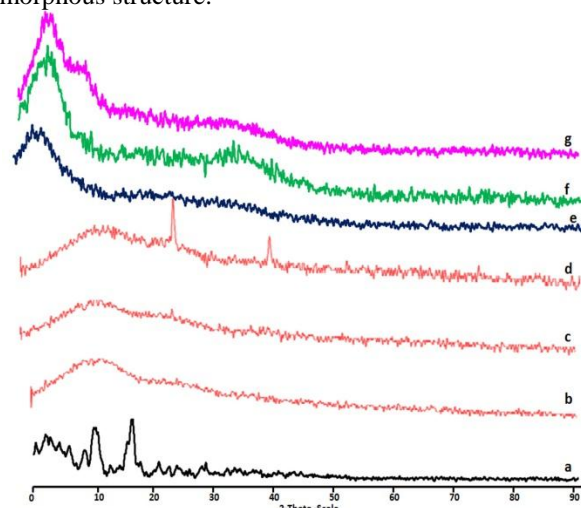


**Figure 3.** XRD thermogram of KF (a); PLGA (b); NS<sub>P1</sub> (KF:PLGA) 1:5 ratio (c); blank NS<sub>P1</sub> (d); Eudragit RL100 (e); NS<sub>E3</sub> (KF:EU) 1:15 ratio (f); blank NS<sub>E3</sub> (g), respectively.

The FT-IR spectrum of KF alone showed that the principal peaks were observed at wave numbers

stretching vibration N-H at  $3424.64\text{ cm}^{-1}$ , aromatic stretching vibration C=C at  $1649.70\text{ cm}^{-1}$ , bending vibration CH<sub>3</sub> at  $1476.99\text{ cm}^{-1}$ , bending vibration phenolic OH at  $1397.14$ , and CH out of plane bending vibrations in substituted ethylenic system (-C=CH- (cis) at  $754.15\text{ cm}^{-1}$  (Figure 4). The spectra obtained by FT-IR for the PLGA are presented in Figure 4. The strong bands in the region between  $1760$  and  $1750\text{ cm}^{-1}$  could be observed, in the spectra, due to the stretch of the carbonyl groups within the PLGA. Moreover, stretching bands are observed because of asymmetric and symmetric C-C(=O)-O vibrations between  $1300$  and  $1150\text{ cm}^{-1}$ . The presence of bands in these regions is of benefit in the characterization of esters. The  $3525$  and  $3459\text{ cm}^{-1}$  bands in the FT-IR spectra for lactide and glycolide are ascribed to moisture in the sample (OH group). The absorption bands between  $3600$  and  $3400\text{ cm}^{-1}$  in the spectra presented in Figure 4, showing the hydroxyl group, indicate that the PLGA copolymers are hydrous. FT-IR studies showed characteristic peaks of KF, confirming the purity of the drug. For NS<sub>P</sub>, stretching vibration N-H is seen at  $3400-3423$ , a stretch of the carbonyl groups at  $1760$ , asymmetric and symmetric C-C(=O)-O vibrations at  $1390$  and bending vibrations in substituted ethylenic system (-C=CH- (cis) at  $725-752\text{ cm}^{-1}$ .

For Eudragit RL 100, in the spectra, the strong bands are observed in the region between  $1150-1190\text{ cm}^{-1}$  and  $1240-1270\text{ cm}^{-1}$ , due to the stretch of carbonyl (ester) groups present in the Eudragit (Figure 4). There are also stretching bands in view of the C(=O) ester vibration at  $1734.01\text{ cm}^{-1}$ . The  $1388.22$ ,  $1449.97$ ,  $2953$ , and  $2992.11\text{ cm}^{-1}$  bands in the FT-IR spectra can be discerned to CH<sub>x</sub> vibration. IR absorption frequency at  $3437.91\text{ cm}^{-1}$  (OH stretch) presented in Figure 3 and showing the hydroxyl group, indicates that the Eudragit RL100 is hydrous.<sup>29,31</sup>

FT-IR spectral studies showed that there was an interaction between KF and polymers used. For NS<sub>E</sub>, stretching strong band C-H (alkyne group) are seen at  $3293.88-3298\text{ cm}^{-1}$ , stretch band strong C-H (alkane group) at  $2936.61$ ,  $2937.50$  and  $2939.24\text{ cm}^{-1}$ , N-H stretch band of the amine group at  $3000\text{ cm}^{-1}$ , stretch band of carbonyl group at  $1728.54$ ,  $1728.79$ , and  $1729.01\text{ cm}^{-1}$ , bending vibrations in -C-H at  $1436.12$ ,  $1436.62$ , and  $1438.91\text{ cm}^{-1}$ , stretch band of ester group C-O at  $1089.41$ ,  $1089.61$ , and  $1090.74\text{ cm}^{-1}$ , and stretch band in -C-Cl at  $844.76$ ,  $845.12$ , and  $845.57\text{ cm}^{-1}$  (Figure 4). The available differences in the positions of the absorption bands of KF were seen in spectra of the prepared formulations, proving the presence of chemical interactions in the solid state between the drug and the polymers (PLGA and Eudragit RL100).

### In vitro dissolution studies

In vitro dissolution data of all best formulations (NS<sub>P</sub> and NS<sub>E</sub>) were compared together. The NS<sub>P</sub> formulation showed that  $82.57\%$  of drug was released in  $480\text{ min}$  (NS<sub>P1</sub>). NaCl increased the solubility of drug by entrapping the KF in the network interstitial spaces of

NaCl molecule and also reducing the particle size. In NSs, increasing the osmotic pressure of W<sub>2</sub> (external phase of second emulsion) directs water migration from W<sub>1</sub> to W<sub>2</sub> as well as a rapid shrinkage of the droplets. This phenomenon results in smaller nanoparticles and increases drug release.

In the NS<sub>E</sub> formulation  $88.82\%$  drug was released in  $480\text{ min}$  (NS<sub>E3</sub>). Increasing the dissolution kinetics of KF from NS<sub>E</sub> may be due to the conversion of the drug from crystalline to amorphous state. Also presence of surfactant (PVA) and co-surfactant (ethanol) in NS<sub>E</sub> reduces the interfacial tension and helps to solubilize the drug in the formulation of NS<sub>E</sub>. According to the literature, the drug release amount and behavior as well as the drug absorption are influenced by the particle size. The particle size of NS<sub>E3</sub> ( $117\text{ nm}$ ) and NS<sub>P1</sub> ( $158\text{ nm}$ ) are the smallest which may be the reason for their highest releases (Figure 5).

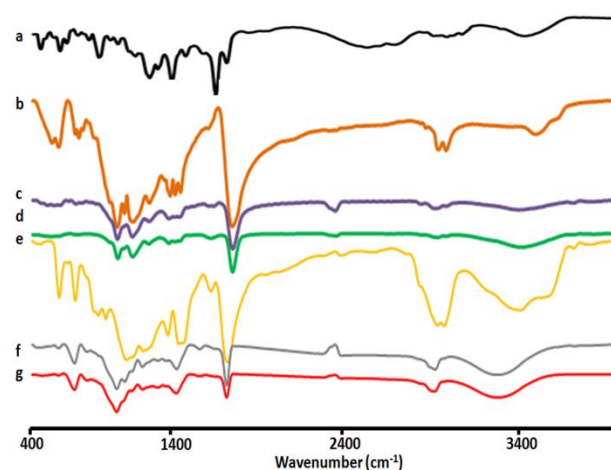


**Figure 4.** FT-IR thermogram of KF (a); PLGA (b); NS<sub>P1</sub> (KF:PLGA) 1:5 ratio (c); blank NS<sub>P1</sub> (d); Eudragit RL100 (e); NS<sub>E3</sub> (KF:EU) 1:15 ratio (f); blank NS<sub>E3</sub> (g), respectively.

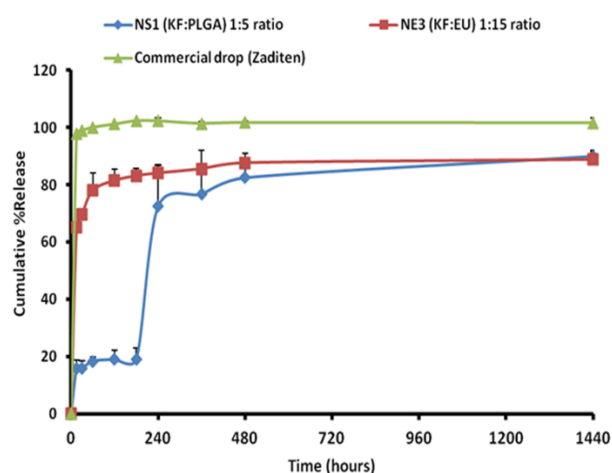


**Figure 5.** Cumulative percent release of KF from nanoparticles with different polymer ratios and KF commercial drop.

KF delivery into and through the bovine cornea was evaluated in *ex vivo* conditions, by the use of Franz vertical diffusion cells. During this study, transcorneal

delivery of prepared KF nanosuspensions was compared with commercial (Zaditen®) eye drop as control. Comparison of data obtained from NS<sub>P</sub> and NS<sub>E</sub> (Table 2) highlights a different KF delivery into and through the bovine cornea. As expected, the NS<sub>E</sub> showed a higher drug permeation and transcorneal delivery than the NS<sub>P</sub>. However, differences of drug permeability in two types of formulations (as NS<sub>P</sub> and NS<sub>E</sub>) were statistically significant ( $p < 0.05$ ). Comparison of data obtained from NS<sub>P</sub> and NS<sub>E</sub> underlines the influence of different formulations on the *ex vivo* drug availability; NS<sub>E</sub> is useful for improving the transcorneal delivery. NS<sub>E</sub> is able to favor KF permeation into the eye and at the same time to prolong the contact time with the cornea and increase the efficacy of drug delivery.

In NSs, solid drug is dissolved in the vehicle (lacrimal fluid) and diffuses through the vehicle to the cornea. On the other side, when a nanocarrier is applied onto the eye, two consecutive physical events may limit corneal absorption, namely, the drug release (from nanocarrier) into lacrimal fluid and its penetration through the corneal barrier. These two processes are intimately intertwined, and both are due to the physicochemical properties of drug (type of nanocarrier) and barrier.

The degree of partitioning of the drug into the cornea relies on the relative affinity for the vehicle and for the intercellular environment. In the present investigation, the higher drug permeability may be due to the polymer type (Table 2), surfactant, and the method of preparation, which taken together act as penetration enhancers.<sup>32,33</sup> In addition, as shown for NS<sub>E</sub>, the small particle size of the NS<sub>E</sub> (in comparison with NS<sub>P</sub>) makes it an excellent carrier for promoting *ex vivo* corneal KF permeation. Overall results show that NS<sub>E</sub> is suitable nanoparticles for corneal delivery of KF. NSs are almost exclusively formed from drug nanoparticles with small amounts of biocompatible and safe surfactants, such as PVA used in this work. This leads to a highly fast dissolution process that favors drug penetration into the cornea. Moreover, compared to other colloidal carriers, NSs show extra advantages such as simplicity, biodegradability of polymer (PLGA), and scalable preparation methods.<sup>34,35</sup>

### Conclusion

On the whole, this work showed the high potential of NS<sub>P</sub> and NS<sub>E</sub> in ocular drug delivery of KF. Indeed, NS<sub>E</sub> has been established to be able to localize the drug into the cornea *ex vivo*. Besides, the NS<sub>P</sub> was shown to give comparable ocular KF delivery as the NS<sub>E</sub>, which strongly enhanced *in vitro* ocular drug delivery. Furthermore, the application of NS<sub>E</sub> in ocular KF delivery showed the advantage of increasing permeability and retention time of the drug in comparison with the NS<sub>P</sub>. To conclude, results of this work evince that NS<sub>E</sub> formulation approach could be a potentially valuable tool of use in the design of new KF nanomedicines for the treatment of eye diseases.

### Acknowledgments

The authors report that they have no conflicts of interests. The financial support from the Drug Applied Research Center of Tabriz University of Medical Sciences under the grant No. 42 is greatly acknowledged. Mitra Jelvehgari received the research grant from Drug Applied Research Center, Tabriz University of Medical Sciences, Tabriz, Iran.

### Ethical Issues

Not applicable.

### Conflict of Interest

The authors declare that there is no conflict of interests regarding the publication of this article.

### References

1. Sahoo SK, Dilnawaz F, Krishnakumar S. Nanotechnology in ocular drug delivery. *Drug Discov Today* 2008;13(3-4):144-51. doi: 10.1016/j.drudis.2007.10.021
2. Patel A, Cholkar K, Agrahari V, Mitra AK. Ocular drug delivery systems: An overview. *World J Pharmacol* 2013;2(2):47-64. doi: 10.5497/wjp.v2.i2.47
3. Ganta S, Paxton JW, Baguley BC, Garg S. Formulation and pharmacokinetic evaluation of an asulacrine nanocrystalline suspension for intravenous delivery. *Int J Pharm* 2009;367(1-2):179-86. doi: 10.1016/j.ijpharm.2008.09.022
4. Adamczak M. Surfactants, polyelectrolytes and nanoparticles as building blocks for nanocarriers. Poland : AGH University of Science and Technology in Krakow; 2013.
5. Jay KT. Nanosuspensions: Types of nanosuspension methods and various applications. Available from: <http://www.biotecharticles.com/Nanotech/2011/May/Nanotechnology-Article/Nanosuspensions-Types-of-Nanosuspension-Methods-and-Variou-Applications-893.html> Article. 2011.
6. Kumari A, Yadav SK, Yadav SC. Biodegradable polymeric nanoparticles based drug delivery systems. *Colloids Surf B Biointerfaces* 2010;75(1):1-18. doi: 10.1016/j.colsurfb.2009.09.001
7. Nagarwal RC, Kant S, Singh PN, Maiti P, Pandit JK. Polymeric nanoparticulate system: A potential approach for ocular drug delivery. *J Control Release* 2009;136(1):2-13. doi: 10.1016/j.jconrel.2008.12.018
8. Patel VR, Agrawal YK. Nanosuspension: An approach to enhance solubility of drugs. *J Adv Pharm Technol Res* 2011;2(2):81-7. doi: 10.4103/2231-4040.82950
9. Mudgil M, Gupta N, Nagpal M, Pawar P. Nanotechnology: a new approach for ocular drug delivery system. *Int J Pharm Pharm Sci* 2012;4(2):105-12.
10. Bangia JK, Om H. Nanoemulsions: a versatile drug delivery tool. *Int J Pharm Sci Res* 2015;6(4):1363-72 doi: 10.13040/IJPSR.0975-8232.6(4).1363-72
11. Mygind T, Stiehler M, Baatrup A, Li H, Zou X, Flyvbjerg A, et al. Mesenchymal stem cell ingrowth

- and differentiation on coralline hydroxyapatite scaffolds. *Biomaterials* 2007;28(6):1036-47. doi: 10.1016/j.biomaterials.2006.10.003
12. James D. Pipkin, Rupert O. Zimmerer, John M. Siebert, inventors; Cydex Pharmaceuticals, Inc., assignee. Nasal and ophthalmic delivery of aqueous corticosteroid solutions. United States patent US20090312724 A1.2009
  13. Aksungur P, Demirbilek M, Denkbas EB, Vandervoort J, Ludwig A, Unlu N. Development and characterization of cyclosporine a loaded nanoparticles for ocular drug delivery: Cellular toxicity, uptake, and kinetic studies. *J Control Release* 2011;151(3):286-94. doi: 10.1016/j.jconrel.2011.01.010
  14. Mandal B, Alexander KS, Riga AT. Sulfacetamide loaded eudragit(r) rl100 nanosuspension with potential for ocular delivery. *J Pharm Pharm Sci* 2010;13(4):510-23.
  15. Gupta H, Aqil M, Khar RK, Ali A, Bhatnagar A, Mittal G. Sparfloxacin-loaded plga nanoparticles for sustained ocular drug delivery. *Nanomedicine* 2010;6(2):324-33. doi: 10.1016/j.nano.2009.10.004
  16. Oshlack B, Pedi Jr F, Chasin M., Inventors; Euro-Celtique SA, assignee. Controlled release formulations coated with aqueous dispersions of acrylic polymers. United States patent US5580578 A. 1996
  17. Mundargi RC, Babu VR, Rangaswamy V, Patel P, Aminabhavi TM. Nano/micro technologies for delivering macromolecular therapeutics using poly(d,l-lactide-co-glycolide) and its derivatives. *J Control Release* 2008;125(3):193-209. doi: 10.1016/j.jconrel.2007.09.013
  18. Danhier F, Ansorena E, Silva JM, Coco R, Le Breton A, Preat V. Plga-based nanoparticles: An overview of biomedical applications. *J Control Release* 2012;161(2):505-22. doi: 10.1016/j.jconrel.2012.01.043
  19. Al-Kassas R. Design and in vitro evaluation of gentamicin-eudragit microspheres intended for intra-ocular administration. *J Microencapsul* 2004;21(1):71-81. doi: 10.1080/02652040310001619992
  20. Pignatello JJ, Oliveros E, MacKay A. Advanced oxidation processes for organic contaminant destruction based on the Fenton reaction and related chemistry. *Crit Rev Environ Sci Tech* 2006;36(1):1-84. doi:10.1080/10643380500326564
  21. Haznedar S, Dortunc B. Preparation and in vitro evaluation of eudragit microspheres containing acetazolamide. *Int J Pharm* 2004;269(1):131-40.
  22. Pignatello R, Bucolo C, Ferrara P, et al. Eudragit RS100® nanosuspensions for the ophthalmic controlled delivery of ibuprofen. *Eur J Pharm Sci* 2002;16(1):53-61. doi:10.1016/S0928-0987(02)00057-X
  23. Dillen K, Vandervoort J, Van den Mooter G, Ludwig A. Evaluation of ciprofloxacin-loaded eudragit rs100 or rl100/plga nanoparticles. *Int J Pharm* 2006;314(1):72-82. doi: 10.1016/j.ijpharm.2006.01.041
  24. Muthu MS, Rawat MK, Mishra A, Singh S. Plga nanoparticle formulations of risperidone: Preparation and neuropharmacological evaluation. *Nanomedicine* 2009;5(3):323-33. doi: 10.1016/j.nano.2008.12.003
  25. Jantarat C. Application of Molecularly Imprinted Polymer for Drug Delivery and Membrane Separation of Chiral Drugs (PhD thesis). Southern Thailand: Prince of Songkla University; 2009.
  26. Meinel L, Illi OE, Zapf J, Malfanti M, Peter Merkle H, Gander B. Stabilizing insulin-like growth factor-i in poly(d,l-lactide-co-glycolide) microspheres. *J Control Release* 2001;70(1-2):193-202.
  27. Hu J, Johnston KP, Williams RO, 3rd. Spray freezing into liquid (sfl) particle engineering technology to enhance dissolution of poorly water soluble drugs: Organic solvent versus organic/aqueous co-solvent systems. *Eur J Pharm Sci* 2003;20(3):295-303.
  28. Ignatious F, Sun L, inventors; Ignatious F, Sun L, assignee. Electrospun amorphous pharmaceutical compositions. United States patent US 20060013869A1. 2006.
  29. Mandal B. Preparation and physicochemical characterization of Eudragit® RL100 Nanosuspension with potential for Ocular Delivery of Sulfacetamide (PhD thesis). Ohio: The University of Toledo Digital Respository; 2010.
  30. Swarnakar NK, Jain AK, Singh RP, Godugu C, Das M, Jain S. Oral bioavailability, therapeutic efficacy and reactive oxygen species scavenging properties of coenzyme q10-loaded polymeric nanoparticles. *Biomaterials* 2011;32(28):6860-74. doi: 10.1016/j.biomaterials.2011.05.079
  31. Basu SK, Adhiyaman R. Preparation and characterization of nitrendipine-loaded Eudragit RL 100 microspheres prepared by an emulsion-solvent evaporation method. *Trop J Pharm Res* 2008;7(3):1033-41.
  32. Kaur IP, Kanwar M. Ocular preparations: The formulation approach. *Drug Dev Ind Pharm* 2002;28(5):473-93. doi: 10.1081/DDC-120003445
  33. Ye T, Yuan K, Zhang W, Song S, Chen F, Yang X, et al. Prodrugs incorporated into nanotechnology-based drug delivery systems for possible improvement in bioavailability of ocular drugs delivery. *Asian J Pharm Sci* 2013;8(4):207-17. doi:10.1016/j.ajps.2013.09.002
  34. Champion JA, Katare YK, Mitragotri S. Particle shape: a new design parameter for micro- and nanoscale drug delivery carriers. *J Control Rel* 2007;121(1):3-9. doi:10.1016/j.jconrel.2007.03.022
  35. Reis CP, Neufeld RJ, Ribeiro AJ, et al. Nanoencapsulation I. Methods for preparation of drug-loaded polymeric nanoparticles. *Nanomed: Nanotech, Bio Med* 2006;2(1):8-21. doi:10.1016/j.nano.2005.12.003